Food and Bioprocess Technology
https://doi.org/10.1007/s11947-024-03690-9

RESEARCH

Analysis of the Induced Mild Heating by Airborne Ultrasound Application on the Convective Drying of Pork Liver

Eduardo A. Sánchez-Torres[1] · Anabella S. Giacomozzi[1] · Blanca Abril[2] · Jose Benedito[1] · Jose Bon[1] · Jose V. García-Pérez[1]

Received: 9 September 2024 / Accepted: 24 November 2024

Abstract

Efficient use of meat by-products, such as pork liver, may entail a previous stage of dehydration for their stabilization, which involves significant energy and time investments. Airborne ultrasound application has been reported as a promising technique to accelerate the air drying of food materials. In this context, the present study addresses, for the first time, the thermal effect associated with ultrasound application on a meat by-product. For that purpose, drying experiments were conducted at 40 and 60 °C on pork liver cylinders at 2 $m \cdot s^{-1}$ with (US) and without (AIR) airborne ultrasound application. The modeling process was based on the principles of heat conduction and moisture diffusion, taking into account the external convection. The results showed that the use of ultrasound reduced the drying time by around 30% at 40 °C, although its impact was less pronounced at 60 °C. With the application of ultrasound, both the sample and air flow temperatures rose by about 4.5 and 2.5 °C, respectively, which partly explains the improvement of drying rate. Due to this low heating effect, airborne ultrasound application must be considered a non-thermal intensification strategy for convective drying of pork liver.

Keywords By-products · Drying · Emerging technologies · Airborne ultrasound · Thermal effect

Nomenclatures

c_p	Specific heat capacity, $J \cdot kg^{-1} \cdot °C^{-1}$
D_e	Effective moisture diffusivity, $m^2 \cdot s^{-1}$
d.b.	Dry basis, kg water·(kg dry solid)$^{-1}$
h	Heat transfer coefficient, $W \cdot m^{-2} \cdot °C^{-1}$
J_0	Bessel function of the first kind of order zero
J_1	Bessel function of the first kind of first order
k	Convective mass transfer coefficient, kg water$\cdot m^{-2} \cdot s^{-1}$
L	Sample half-thickness, m
M	Number of model parameters
MRE	Mean relative error, %
N	Number of experimental data
R	Sample radius, m
r	Radial direction, m
S_y	Standard deviation of the sample, units of the sample
S_{yx}	Standard deviation of the estimation, units of the estimation
T	Solid temperature, °C
T_0	Initial solid temperature, °C
t	Drying time, s
T_∞	Drying air temperature, °C
VAR	Explained variance, %
W	Moisture content of sample, kg water·(kg dry solid)$^{-1}$
W_0	Initial moisture content of sample, kg water·(kg dry solid)$^{-1}$
W_e	Equilibrium moisture content, kg water·(kg dry solid)$^{-1}$
W_p	Local moisture content, kg water·(kg dry solid)$^{-1}$
$\overline{y_{\exp}}$	Average of experimental data, units of the data
$y_{i\,\mathrm{calc}}$	Estimated data i, units of the data
$y_{i\,\exp}$	Experimental data i, units of the data
z	Axial direction, m

Highlights
- The airborne application of power ultrasound shortened the drying time by up to 30% at 40 °C.
- The ultrasonic effect on drying kinetics was reduced at high temperatures.
- The ultrasound application increased both the effective diffusivity and the mass transfer coefficient.
- Airborne ultrasonic drying may be considered a non-thermal intensification strategy due to its low heating effect.

✉ Jose V. García-Pérez
jogarpe4@tal.upv.es

[1] Institute of Food Engineering–FoodUPV, Universitat Politècnica de València, Valencia, Spain

[2] Agrifood Research and Technology Centre of Aragon (CITA), Zaragoza, Spain

Published online: 02 January 2025

α	Thermal diffusivity, $m^2 \cdot s^{-1}$
λ_n	Roots of the Bessel function of the first kind of order zero
φ_{air}	Relative humidity of air
φ_e	Relative humidity of equilibrium
ρ	Solid density, $kg \cdot m^{-3}$
ρ_{ds}	Dry solid density, $kg \cdot m^{-3}$

Introduction

The meat industry produces a significant amount of edible animal co-products that currently have low commercial value due to changing consumption trends. Among these co-products, pork liver represents a potential source of high-quality proteins that can be utilized as ingredients in the food processing sector. However, the high perishability of pork liver poses handling challenging (Henchion & McCarthy, 2019), making moisture depletion a suitable preliminary step for its stabilization. Dehydration provides not only stabilization of the raw liver but also concentration of its protein content. Hence, through a simple dehydration process, pork liver turns into a protein concentrate with about 70% protein, offering a novel ingredient for use in food formulations. Although hot air drying is the simplest and most affordable technique for reducing moisture content, it does demand a substantial quantity of energy and time, which justifies the use of novel technologies for its intensification (Sánchez-Torres et al., 2022). Nonetheless, previous studies have reported how the protein fraction of pork liver is degraded by high temperatures during convective drying. As a result, different physicochemical and techno-functional properties of pork liver were affected as the air temperature increased (Abril et al., 2022b). Moreover, the use of high drying temperatures also disturbed the ferrochelatase activity for the formation of zinc protoporphyrin (ZnPP) in pork liver (Abril et al., 2022a). ZnPP possesses technological significance because it is red and highly resistant to light and heat, which can enhance the attractiveness of meat products while avoiding or reducing the debated addition of nitrites/nitrates (Llauger et al., 2023; Wakamatsu, 2022). Therefore, the search for emerging technologies for the enhancement of pork liver drying should be based on non-thermal intensification mechanisms, permitting the acceleration of the process within the range of mild drying temperatures.

Liquid-borne ultrasound pretreatment prior to air drying has been widely studied in the dehydration of fruits and vegetables with the goal of increasing the drying rate by improving internal moisture diffusion (Deng et al., 2019). The ultrasound pretreatment, together with the application of mild drying temperatures, allows the degradation of thermolabile compounds to be minimized while shortening drying times (Llavata et al., 2020). Nevertheless, during ultrasound pretreatment, the food material is immersed in a liquid, such as gel, water, or oil for the treatment. Thus, two main aspects have to be considered due to ultrasound causes: (i) structural damage to the food tissue facilitating leakage of food components to the liquid (Mieszczakowska-Frąc et al., 2016) and (ii) the product may be contaminated by the liquid medium or its organoleptic characteristics may be altered (Miano et al., 2016). In this context, the development of airborne ultrasonic transducers has garnered increasing interest for their use in air drying processes (Andrés et al., 2019). Therefore, airborne ultrasound-assisted drying has emerged as a novel non-thermal technology aimed at enhancing heat and mass transfer mechanisms, affecting both diffusion and convective transport during water removal (Villamiel et al., 2021). When airborne power ultrasound is applied during convective drying, the ultrasonic wave is transmitted from the transducer into the air and finally reaches the product to be dried. Thus, the ultrasonic wave causes alternating compressions and expansions inside the food matrix (sponge effect), which involves a mechanical stress that enhances the internal moisture diffusion, facilitating the water removal (Miraei Ashtiani et al., 2022). At the same time, the compressions and expansions of the surrounding air at the solid–gas interface promote external convective moisture transport, as a consequence of the reduction in the boundary layer thickness (Llavata et al., 2024). Additionally, it has previously been described how the application of ultrasound is also able to enhance heat transport by both conduction (Contreras et al., 2018) and convection (Musielak & Mierzwa, 2021). Compared to ultrasonic pretreatment in liquid medium, the structural effect on the food solid matrix linked to the airborne ultrasound application is moderate (García-Pérez et al., 2012, 2023).

Although power ultrasound is commonly recognized as a non-thermal technology in food engineering (Jadhav et al., 2021), several investigations have found a certain thermal effect when ultrasound is applied during convective drying. Thereby, a significant temperature increase induced by the use of ultrasound has been reported in both the product (Colucci et al., 2018) and the drying air (García-Pérez et al., 2013) although there is a lack of consensus as to how ultrasound induces heating in the product. The internal friction generated by the ultrasonic wave during the alternating compressions and expansions of the solid matrix might be transformed into thermal energy, explaining the increase in product temperature. Even above a certain level of acoustic energy, the ultrasonic cavitation bubbles might also contribute to the temperature rise to some extent. Therefore, this thermal effect associated with ultrasound application should be carefully assessed in the drying of heat-sensitive matrices. Furthermore, Ozuna et al. (2014b) demonstrated that the effectiveness of airborne power ultrasound is heavily dependent on the structure of the material to be dried. Thus, these authors evidenced that materials with a soft and porous structure exhibit

a better transmission of acoustic energy from the air. In contrast, hard and compact product structures are less affected by acoustic energy, since the substantial impedance differences between the product and the air lead to a significant energy loss at the interface. In addition, the product structure will also control the energy loss in the ultrasonic wave by attenuation, which would result in a certain heating. Hence, the thermal effect found may be greater or lesser depending on the type of food matrix. To our knowledge, the thermal effect of airborne ultrasound on meat matrices or their related by-products has not been previously described. Thus, the aim of this study was to analyze the influence of airborne ultrasound application on joint heat and mass transfer during the hot air drying of pork liver. The modeling process considered the theory of heat conduction and moisture diffusion, assessing the contribution of the external convection.

Materials and Methods

Sample Shaping

Fresh pork livers were acquired from a slaughterhouse located in Valencia, Spain. The livers were first separated into four portions according to their primary lobes. Afterward, each portion was vacuum packed (SU-604, Sammic, Gipuzkoa, Spain), frozen in a blast chiller (ABT71L, Infrico Supermarket, Córdoba, Spain) and stored at − 20 °C until required. Before every drying experiment, cylindrical samples (12.6 mm in diameter and 15 mm in height) of pork liver were obtained using a hollow punch.

Drying Experiments

The drying experiments were performed in a convective dryer with PID control of temperature and air velocity, as already described in the literature (Cruz et al., 2016; García-Pérez et al., 2013). An ultrasound excited cylinder (internal diameter 100 mm, height 310 mm, and thickness 10 mm) coupled to a piezoelectric transducer (21.5 kHz) constitutes the drying chamber in which the samples are placed and the air flows through them, as illustrated in Fig. 1.

The drying kinetics were carried out at 2 $m \cdot s^{-1}$ testing two temperatures, 40 and 60 °C, without (AIR) and with (US) ultrasonic application. Both mass loss and temperature were automatically recorded at different preset times. Specifically, the temperature was measured in the air flow at the inlet and outlet of the drying chamber and in the center of two liver cylinders (Fig. 1), using J-type thermocouples connected to a data acquisition unit (34970A, Agilent Technologies, Inc., California, USA). Thereby, the temperature measurement in the sample was performed on two liver cylinders positioned at two different points (10 and 20 cm from the air inlet) and

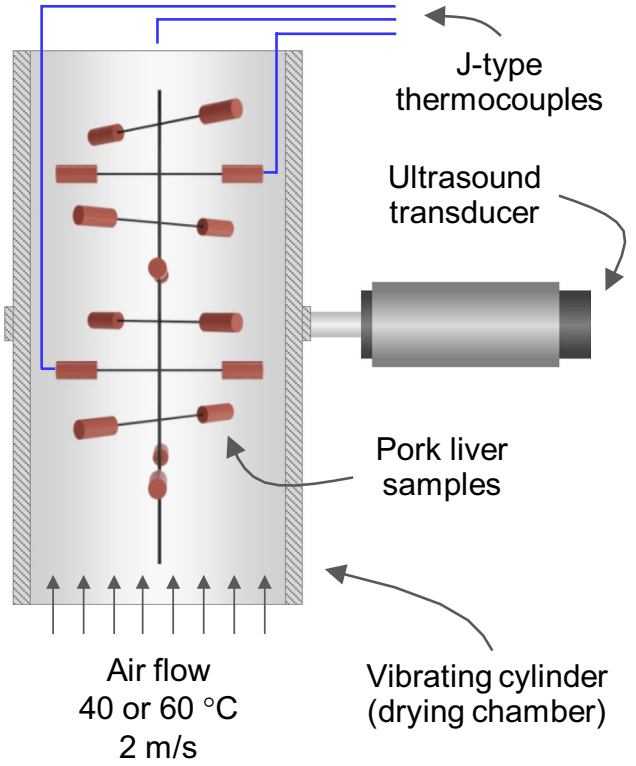

Fig. 1 Ultrasonically assisted drying chamber. Detail of pork liver samples and placement of J-type thermocouples

averaged. Likewise, the temperature of the air flow was monitored at the inlet and outlet of the drying chamber in order to assess the temperature variation. Meanwhile, the mass loss was recorded by means of a balance (PM4000, Mettler-Toledo, Greinfensee, Switzerland) attached to the sample holder. The relative humidity and temperature of the room air were also monitored (TFG 80, Galltec + Mela, Bondorf, Germany). For the US experiments, 50 W of electrical power was provided to the ultrasonic transducer. The drying tests were prolonged until the samples lost 70% of their initial weight (30 ± 1 g), considering at least three replicates per experimental condition.

Mathematical Modeling

The mathematical description of the drying process focused on modeling heat and mass transport phenomena according to the principles outlined in the Fourier and Fick laws, respectively. The governing equations used, corresponding to a finite cylindrical geometry, are defined below:

$$\frac{\partial T(r,z,t)}{\partial t} = \alpha\left(\frac{\partial^2 T(r,z,t)}{\partial r^2} + \frac{\partial^2 T(r,z,t)}{\partial z^2} + \frac{1}{r}\frac{\partial T(r,z,t)}{\partial r}\right) \quad (1)$$

$$\frac{\partial W_p(r,z,t)}{\partial t} = D_e\left(\frac{\partial^2 W_p(r,z,t)}{\partial r^2} + \frac{\partial^2 W_p(r,z,t)}{\partial z^2} + \frac{1}{r}\frac{\partial W_p(r,z,t)}{\partial r}\right) \quad (2)$$

Thus, both the thermal diffusivity (α) and the effective moisture diffusivity (D_e) were assumed to be constant within the examined period. The governing equations (Eqs. (1) and (2)) were solved neglecting (NER model) or considering (ER model) the external resistance to heat and mass transfer, depending on the boundary conditions used in each case (Cárcel et al., 2007; Contreras et al., 2018; García-Pérez et al., 2006).

NER Model

If the external resistance is neglected, it is assumed that the cylindrical surface instantaneously reaches the equilibrium air temperature and moisture, and therefore, the following boundary conditions are necessary for each characteristic direction (r, z):

If $t > 0$ and $r = R$ such that $r \in [0, R]$, then

$$T(R, z, t) = T_\infty \tag{3}$$

$$W_p(R, z, t) = W_e \tag{4}$$

If $t > 0$ and $z = L$ such that $z \in [0, L]$, then

$$T(r, L, t) = T_\infty \tag{5}$$

$$W_p(r, L, t) = W_e \tag{6}$$

Considering these boundary conditions, the governing equations (Eqs. (1) and (2)) can be solved analytically by applying the method of variable separation. Thus, Eqs. (7) and (8) show the solution of the heat and mass transport governing equations, respectively, assuming the boundary conditions indicated in Eqs. (3) to (6).

$$\begin{aligned} T(r,z,t) &= T_\infty + \left(T_0 - T_\infty\right) \\ &\times \left[\sum_{n=1}^{\infty} \frac{2}{\lambda_n J_1(\lambda_n)} \exp\left(-\frac{\alpha \lambda_n{}^2 t}{R^2}\right) J_0\left(\frac{\lambda_n r}{R}\right)\right] \\ &\times \left[\sum_{n=0}^{\infty} \frac{4(-1)^n}{(2n+1)\pi} \exp\left(-\frac{\alpha(2n+1)^2\pi^2 t}{4L^2}\right) \cos\left(\frac{(2n+1)\pi}{2L} z\right)\right] \end{aligned} \tag{7}$$

$$\begin{aligned} W(t) &= W_e + \left(W_0 - W_e\right) \\ &\times \left[\sum_{n=1}^{\infty} \frac{4}{\lambda_n{}^2} \exp\left(-\frac{D_e \lambda_n{}^2 t}{R^2}\right)\right] \\ &\times \left[\sum_{n=0}^{\infty} \frac{8}{(2n+1)^2\pi^2} \exp\left(-\frac{D_e(2n+1)^2\pi^2 t}{4L^2}\right)\right] \end{aligned} \tag{8}$$

The thermal diffusivity (α) and the effective moisture diffusivity (D_e) were identified through the minimization of the sum of squared errors between the observed temperature-moisture data and the computed values, respectively. For this goal, the *alabama* algorithm from the ROI package (Theußl et al., 2017) within the R programming environment (v. 4.3.3) (R Core Team, 2022) was applied. The equilibrium moisture content (W_e) was calculated using the desorption isotherms of pork liver that were previously reported by Sánchez-Torres et al. (2021).

ER Model

When external resistance to heat and mass transfer is considered, the boundary conditions specified in Eqs. (3) to (6) are substituted by Eqs. (9) to (12), respectively. These new assumptions compute the convective flow of heat or mass at the air–solid interface:

If $t > 0$ and $r = R$ such that $r \in [0, R]$, then

$$-\alpha \rho c_p \frac{\partial T(R, z, t)}{\partial r} = h(T(R, z, t) - T_\infty) \tag{9}$$

$$-D_e \rho_{ds} \frac{\partial W_p(R, z, t)}{\partial r} = k\left(\varphi_e(R, z, t) - \varphi_{\text{air}}\right) \tag{10}$$

If $t > 0$ and $z = L$ such that $z \in [0, L]$, then

$$-\alpha \rho c_p \frac{\partial T(r, L, t)}{\partial z} = h(T(r, L, t) - T_\infty) \tag{11}$$

$$-D_e \rho_{ds} \frac{\partial W_p(r, L, t)}{\partial z} = k\left(\varphi_e(r, L, t) - \varphi_{\text{air}}\right) \tag{12}$$

Assuming these new boundary conditions, an analytical solution for the mass transport governing equation (Eq. (2)) cannot be obtained, requiring instead the use of a numerical solution. In the case of the heat transport governing equation (Eq. (1)), the analytical solution requires iterative calculations, which greatly increases the computing requirements. For this reason, and due to the existing analogy between the governing equations and the initial and boundary conditions for both cases (heat and mass transfer), the ER model was solved numerically using the finite element method through COMSOL Multiphysics software (v. 3.4, COMSOL Inc., Burlington, MA, USA).

Afterward, the values of the thermal diffusivity (α), the effective moisture diffusivity (D_e), and the heat (h) and mass (k) external transfer coefficients were determined from a non-linear optimization procedure. To this end, the *surrogateopt* function from the MATLAB environment (v. R2023b, The MathWorks Inc., Natick, MA, USA) was applied. The objective function was likewise the sum of the squared errors between the observed and computed data.

Goodness-of-Fit

The mean relative error (MRE, Eq. (13)) and the explained variance (VAR, Eq. (14)) were computed in order to assess how well each model fits the observed data.

$$\mathrm{MRE} = \frac{100}{N}\sum_{i=1}^{N}\frac{\left|y_{i\,\mathrm{exp}} - y_{i\,\mathrm{calc}}\right|}{y_{i\,\mathrm{exp}}} \tag{13}$$

$$\mathrm{VAR} = \left(1 - \frac{S_{yx}^2}{S_y^2}\right)100 \tag{14}$$

where

$$S_y = \sqrt{\frac{1}{N-1}\sum_{i=1}^{N}\left(y_{i\,\mathrm{exp}} - \overline{y_{\mathrm{exp}}}\right)^2} \tag{15}$$

$$S_{yx} = \sqrt{\frac{1}{N-M}\sum_{i=1}^{N}\left(y_{i\,\mathrm{exp}} - y_{i\,\mathrm{calc}}\right)^2} \tag{16}$$

Statistical Analysis

To evaluate the impact of the air temperature and the ultrasound application on the model parameters, i.e., diffusivities and transfer coefficients, a multifactor analysis of variance (ANOVA) was performed. The mean comparisons were conducted using LSD (least significant difference) intervals, with a confidence level of 95%. The statistical computations were carried out using the R programming language (v. 4.3.3) (R Core Team, 2022).

Results and Discussion

Experimental Drying Kinetics

The experimental drying kinetics of pork liver at 40 and 60 °C without (AIR) and with ultrasound application (US) are shown in Fig. 2. The drying rate (dW/dt) was approached to $\Delta W/\Delta t$ for every pair of consecutive observations, allowing different dehydration periods to be identified. No period of constant drying rate was found for any of the experimental conditions tested, which emphasizes the importance of internal transport as a key aspect in the control of pork liver drying. Thereby, this suggests that the critical moisture content coincides with the initial moisture content. Similar observations have been reported in the convective drying of protein-rich products, such as pork (Clemente et al., 2011), beef (Muga et al., 2020), or catfish (Mujaffar & Sankat, 2015).

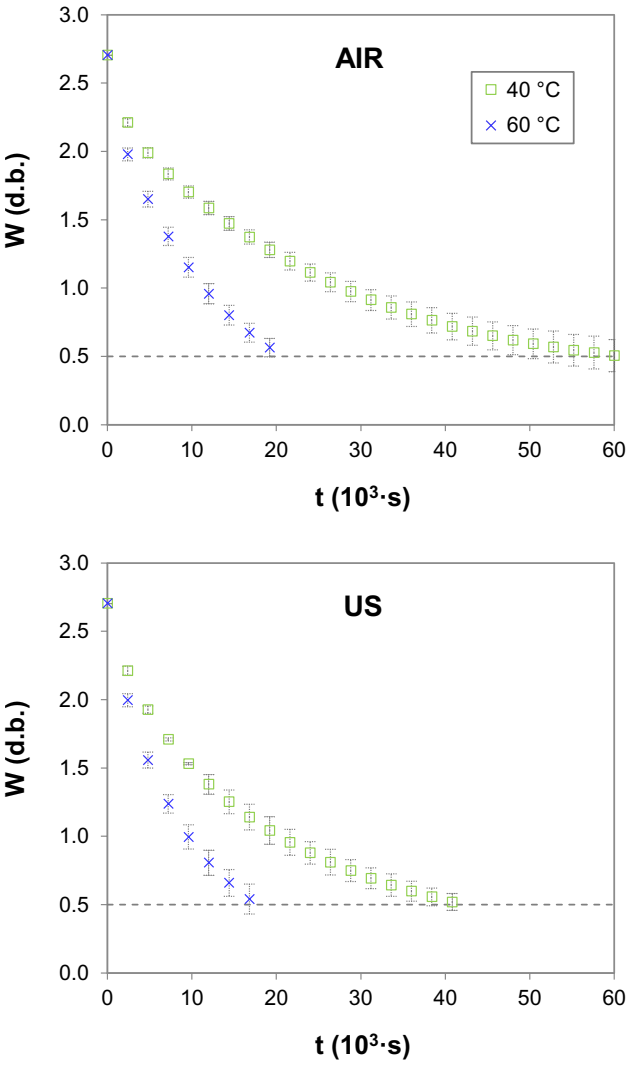

Fig. 2 Experimental moisture content of pork liver in relation to drying time without (AIR) and with (US) ultrasound application at 40 and 60 °C. Error bars show standard deviation

The effect of the drying temperature was evidenced in both the AIR and US sets (Fig. 2). Specifically, achieving a moisture content of 0.5 d.b. in the AIR experiments necessitated approximately 17 h at 40 °C, whereas drying at 60 °C was accomplished in only 6 h. In the US experiments, the application of ultrasound resulted in a discernible enhancement in the drying rate at 40 °C. Consequently, the duration required to reach a moisture content of 0.5 d.b. was reduced to 12 h compared to the 17 h necessary in the AIR set. This reduction translates to a decrease in drying time of almost 30%, aligning with findings documented for other protein-rich products, such as fish. For example, in cod drying at 20 °C, Bantle and Hanssler (2013) found that the drying time was around 32% shorter, while a slightly higher figure, of

approximately 40%, was reported by Ozuna et al. (2014a). Meanwhile, the application of airborne ultrasound during the drying process of fruits and vegetables has resulted in greater drying time reductions, ranging from 60 to 80% (García-Pérez et al., 2023), which highlights the role of the product structure on the effectiveness of power ultrasound. As already discussed, Ozuna et al. (2014b) demonstrated that soft and porous product structures are more susceptible to airborne ultrasonic application than hard and compact structures due to (i) higher transmission coefficients at the air interface, (ii) greater attenuation, and (iii) less mechanical resistance.

In the drying experiments at 60 °C, the impact of ultrasound was of a lesser magnitude (the drying time was shorter by close to only 10%), as illustrated in Fig. 2. The fact that ultrasound application is less effective at high drying temperatures has previously been reported in other products, such as carrots (García-Pérez et al., 2006), apple (Rodríguez et al., 2014), or cod (Bantle & Hanssler, 2013). Thereby, García-Pérez et al. (2006) suggested that the higher the thermal energy, the minor the contribution of acoustic energy to water mobility. In addition, the higher the air temperature, the higher the ultrasonic attenuation. In this sense, Jakevičius and Demčenko (2008) showed attenuation coefficients of approximately 1.2 and 1.8 $dB \cdot m^{-1}$ at 40 and 60 °C (at 50 kHz and 20% relative humidity), respectively. The aforementioned aspects explained the milder effect of ultrasound at 60 than 40 °C.

As for the heat transport, the temperature profiles at the center of the sample and the outlet of the drying chamber are shown in Figs. 3 and 4, respectively, for the different experimental conditions tested. In the AIR experiments, the highest temperature recorded at the center of the sample was 35.59 ± 0.45 °C at 40 °C and 52.38 ± 0.48 °C at 60 °C. Thus, within the examined range, the center of the sample did not reach the designated set point temperature (± 0.1 °C) in any instance, due to the continual evaporation of solid moisture content during the drying process. When ultrasound was applied, a temperature rise was found at the center of the sample across the entire temperature profile (Fig. 3), peaking at 40.12 ± 0.33 °C at 40 °C and 56.11 ± 0.25 °C at 60 °C. This denotes an increase in the maximum temperature at the center of the sample by 4.53 and 3.73 °C, respectively, attributed to the ultrasound application. The observed temperature increase may be linked to both the improvement of conduction and convection mechanisms and heat generation due to acoustic attenuation. The enhancement in heat transport facilitated by ultrasound application has been documented in protein matrices, as evidenced in previous research on ham (Contreras et al., 2018). The analysis at the drying chamber outlet (Fig. 4) revealed a temperature rise in the drying air of 2.44 °C at 40 °C and 2.56 °C at 60 °C, slightly less pronounced than that observed within the sample. This increment is likely attributed to heat generation resulting from the partial absorption of ultrasonic waves in the air, or from heat radiation emitted from the cylinder wall.

The temperature increase provoked by the application of airborne ultrasound has also been observed during the convective drying of other food matrices, both in the product and in the air flow. For instance, during the drying of cod, Bantle and Hanssler (2013) reported an increase in the product temperature of close to 5 °C for all the drying temperatures analyzed (10, 20, and 30 °C). Likewise, for the drying of eggplant at − 8 °C, Colucci et al. (2018) identified that the thermal effect of ultrasound on the product was dependent on sample size (17.6 and 8.8 mm side cubes). The larger samples exhibited a higher temperature increase than the smaller ones, around 10 and 5 °C, respectively. The authors considered that the amount of acoustic energy absorbed by each type of sample could be different, being related to the volume of the product. Nonetheless, it is worth mentioning that in both the Bantle and Hanssler (2013) and Colucci et al. (2018) studies, the temperature increase found in the product implied exceeding the set point temperature of the drying air. This reflects that at least part of the ultrasonic energy absorbed by the product was transformed into heat, raising the temperature of the solid. In this sense, Kowalski (2018) compared the thermal effect of ultrasound with its

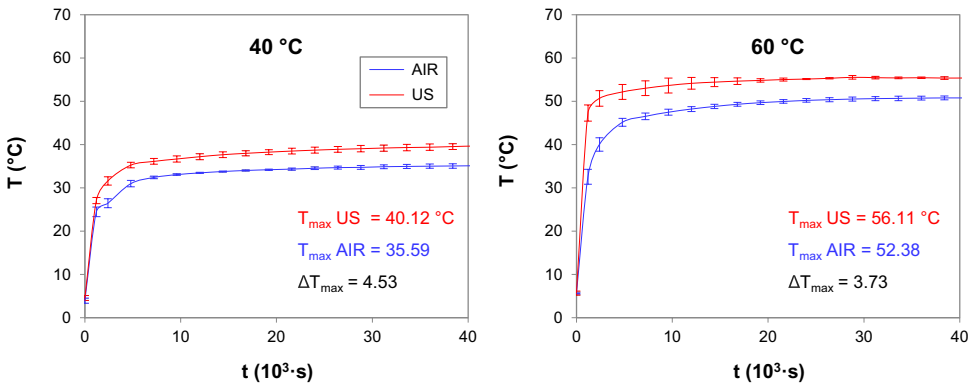

Fig. 3 Temperature in the center of the sample during the drying of pork liver cylinders without (AIR) and with (US) ultrasound application at 40 and 60 °C. Continuous lines show the average values and error bars, the standard deviation

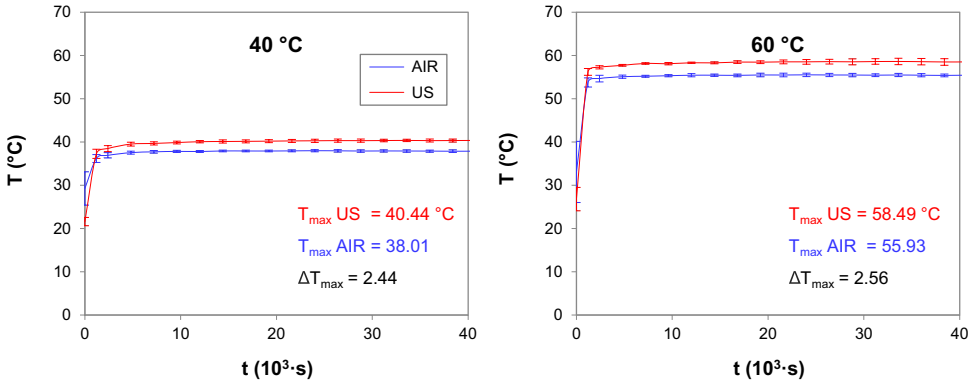

Fig. 4 Drying air temperature at the chamber outlet during the drying of pork liver cylinders without (AIR) and with (US) ultrasound application at 40 and 60 °C. Continuous lines show the average values and error bars, the standard deviation

vibration effect during the airborne ultrasound-assisted drying of strawberries. The study concluded that the vibration effect had a greater impact on the improvement in drying efficiency compared to the identified thermal effect (increase in the temperature of the material of up to 5 °C). Regarding the thermal effect of ultrasound on the drying air, García-Pérez et al. (2013) found an increase in the temperature of the air flow when ultrasound was used in grape stalk drying, which ranged between 5 and 10 °C depending on the ultrasonic power applied, 45 or 90 W, respectively. The low porosity of the stalk could reduce the absorption of acoustic energy, resulting in an increase in the energy available in the gaseous medium. This surplus energy has the potential to be transformed into heat, contributing to an increase in air temperature. In contrast, none of the above-mentioned studies, Bantle and Hanssler (2013), Colucci et al. (2018), or Kowalski (2018), reported a significant rise in the temperature of the drying air using comparable ultrasonic powers.

Thus, the literature confirms that assessing the thermal effect of airborne ultrasound is a complex process that depends on several factors, such as product structure, size, or applied ultrasonic power, and therefore, the application of power ultrasound on the drying of heat-sensitive matrices should be carefully addressed.

NER Model

The NER model focused on describing the internal transport of moisture and heat in pork liver while assuming that the external resistance is negligible. Thus, the identified effective moisture diffusivity (D_e) and thermal diffusivity (α) are shown in Table 1. As anticipated, raising the temperature from 40 to 60 °C caused an increase in effective moisture diffusivity, ranging from 1.04 to 2.20×10^{-10} $m^2 \cdot s^{-1}$. Additionally, the application of ultrasound resulted in higher effective moisture diffusivity figures at both 40 and 60 °C, with values of 1.43 and 2.78×10^{-10} $m^2 \cdot s^{-1}$, respectively. Hence, both the increase in temperature and the application of ultrasound significantly ($p < 0.05$) affected the effective moisture diffusivity, improving the moisture transport by diffusion. However, it should be noted that the effective moisture diffusivity identified by the NER model is, in fact, a kinetic fitting parameter that includes the influence of both diffusion and convective moisture transport. Thereby, an increase in the effective moisture diffusivity could be related to a decrease in both the internal and external resistance. Nonetheless, the enhancement of moisture internal transport as a result of the use of airborne ultrasound has been well documented during the convective drying of many foodstuffs, including protein-rich matrices such as fish (Ozuna et al., 2014a).

Table 1 Effective moisture diffusivity (D_e) and thermal diffusivity (α) estimated using the model that neglects the external resistance (NER) for AIR and US experiments at 40 and 60 °C and statistical fitting parameters: average explained variance (VAR) and mean relative error (MRE)

	AIR	US
Moisture transport		
40 °C		
$D_e \times 10^{10}$ ($m^2 \cdot s^{-1}$)	1.04 ± 0.08^{a}	1.43 ± 0.13^{b}
VAR (%)	97.31	96.38
MRE (%)	6.81	8.23
60 °C		
$D_e \times 10^{10}$ ($m^2 \cdot s^{-1}$)	2.20 ± 0.20^{c}	2.78 ± 0.01^{d}
VAR (%)	94.98	98.47
MRE (%)	10.30	4.70
Heat transport		
40 °C		
$\alpha \times 10^{8}$ ($m^2 \cdot s^{-1}$)	2.78 ± 0.71^{A}	2.81 ± 0.32^{A}
VAR (%)	97.84	97.18
MRE (%)	6.76	7.62
60 °C		
$\alpha \times 10^{8}$ ($m^2 \cdot s^{-1}$)	3.17 ± 0.60^{A}	3.02 ± 0.45^{A}
VAR (%)	97.95	96.58
MRE (%)	4.77	7.31

Average of D_e and $\alpha \pm$ standard deviation ($N = 3$). Superscripts show homogeneous groups established from LSD (least significant difference) intervals ($p < 0.05$) for each kinetic parameter

As for the thermal diffusivity, its value remained around an average of $2.95 \pm 0.18 \times 10^{-8}$ $m^2 \cdot s^{-1}$ for all the experimental conditions tested (Table 1). Hence, neither the increase in drying temperature from 40 to 60 °C nor the application of ultrasound had a significant ($p > 0.05$) impact on the thermal diffusivity. This contradicts the results reported by other studies, which showed that both conduction and convection heat transfer were enhanced through the application of ultrasound. In this sense, Contreras et al. (2018) found that the use of airborne ultrasound during the mild thermal treatment of dry-cured ham with hot air increased thermal diffusivity by up to 37%.

The NER model showed a limited capacity to describe both moisture and heat transport, as evidenced by the low explained variance (VAR) and high mean relative error (MRE) values obtained (Table 1). Thus, the explained variance (VAR) ranged from 94 to 99% for moisture transport and from 96 to 98% for heat transport, while the mean relative error (MRE) reached values close to 10% in several cases. Therefore, a more complex model assuming external resistance should be addressed to achieve a more accurate mathematical description of the moisture and heat transport during the convective drying of pork liver.

ER Model

The ER model considered both internal and external moisture and heat transport, which made it possible to determine the effective moisture diffusivity (D_e) and the thermal diffusivity (α), as well as the mass (k) and heat (h) external transfer coefficients (Table 2). The modeling of moisture transport through the ER model exhibited a satisfactory goodness-of-fit compared to the NER model, with an explained variance (VAR) of more than 99% and a mean relative error (MRE) of less than 5% in every case. These results indicate that the assumption of external resistance to mass transfer is essential under the drying conditions analyzed. Thus, the effective moisture diffusivity ranged from 1.83 to 4.48×10^{-10} $m^2 \cdot s^{-1}$ and the mass transfer coefficient from 4.64 to 11.27×10^{-4} $kg \cdot m^{-2} \cdot s^{-1}$, which are comparable to values found in the literature for other food products (Erbay & Icier, 2010; Fan et al., 2017).

In both the AIR and US experiments, raising the drying air temperature from 40 to 60 °C resulted in an increase in the effective moisture diffusivity and the mass transfer coefficient. Furthermore, the application of ultrasound at 40 °C led to higher figures for both kinetic parameters. However, at 60 °C, the use of ultrasound only involved an increase in the mass transfer coefficient, without affecting the values of the effective moisture diffusivity. As discussed in the "Experimental Drying Kinetics" section, this phenomenon is attributed to (i) the decrease in the relative importance of ultrasonic energy in internal water mobility at high thermal energy levels and (ii) the rise in ultrasonic attenuation as air temperature increases. Hence, both the increase in the drying air temperature and the ultrasound application resulted in a significant ($p < 0.05$) increase in the effective moisture diffusivity and the mass transfer coefficient in pork liver. This shows a decrease in internal and external mass transfer resistance, respectively. Similarly, the improvement in both diffusion and convective mass transport induced by the use of airborne ultrasound has previously been described in the case of the drying of other protein-rich matrices, such as cod (Bantle & Eikevik, 2014), as well as a wide variety of fruits and vegetables (Yao, 2016).

As for the heat transport modeling, Table 2 shows the identified values of thermal diffusivity and heat transfer coefficient. In this case, the ER model did not demonstrate an optimal fit to the experimental temperature data since the explained variance (VAR) ranged from 94 to 98% and the mean relative error (MRE) from 6 to 12%, approximately. Thus, the fitting ability obtained was similar to that found in the NER model. Nevertheless, contrary to the results of the NER model, the rise in the drying air temperature from 40 to 60 °C significantly ($p < 0.05$) affected the thermal diffusivity

Table 2 Effective moisture diffusivity (D_e), thermal diffusivity (α) and mass (k) and heat (h) transfer coefficients identified using the model that considers the external resistance (ER) for AIR and US experiments at 40 and 60 °C and statistical fitting parameters: average explained variance (VAR) and mean relative error (MRE)

	AIR	US
Moisture transport		
40 °C		
$D_e \times 10^{10}$ ($m^2 \cdot s^{-1}$)	1.83 ± 0.43^{a}	2.99 ± 0.02^{b}
$k \times 10^{4}$ ($kg \cdot m^{-2} \cdot s^{-1}$)	4.64 ± 0.58^{y}	5.66 ± 0.81^{y}
VAR (%)	99.16	99.34
MRE (%)	4.51	3.66
60 °C		
$D_e \times 10^{10}$ ($m^2 \cdot s^{-1}$)	4.48 ± 0.39^{c}	4.43 ± 0.39^{c}
$k \times 10^{4}$ ($kg \cdot m^{-2} \cdot s^{-1}$)	6.44 ± 0.63^{y}	11.27 ± 2.54^{z}
VAR (%)	99.40	99.33
MRE (%)	3.35	3.55
Heat transport		
40 °C		
$\alpha \times 10^{8}$ ($m^2 \cdot s^{-1}$)	6.46 ± 1.97^{A}	6.57 ± 0.68^{AB}
h ($W \cdot m^{-2} \cdot °C^{-1}$)	90.83 ± 28.93^{Z}	90.76 ± 9.76^{Z}
VAR (%)	95.87	94.74
MRE (%)	10.46	11.71
60 °C		
$\alpha \times 10^{8}$ ($m^2 \cdot s^{-1}$)	8.47 ± 1.67^{C}	8.41 ± 1.13^{BC}
h ($W \cdot m^{-2} \cdot °C^{-1}$)	88.38 ± 23.51^{Z}	92.16 ± 16.45^{Z}
VAR (%)	97.55	95.64
MRE (%)	6.38	10.07

Average of D_e, k, α, and $h \pm$ standard deviation ($N = 3$). Superscripts show homogeneous groups established from LSD (least significant difference) intervals ($p < 0.05$) for each kinetic parameter

identified by the ER model, which slightly increased its value at 60 °C in both AIR and US experiments. Therefore, between 40 and 60 °C, the thermal diffusivity ($\times 10^{-8}$ $m^2 \cdot s^{-1}$) ranged from 6.46 to 8.47 and from 6.57 to 8.41 for the AIR and US experiments, respectively. These values are in the order of magnitude of those found in the literature for different protein-rich matrices, such as turkey ham (Ayadi et al., 2009), pork loin (Rinaldi et al., 2010), or cod mince (Nesvadba & Eunson, 1984). What has already been observed, furthermore, is the temperature dependence of the thermal diffusivity (Abbas et al., 2008), which is mainly related to changes in the specific heat of the material as the temperature increases. Meanwhile, the heat transfer coefficient remained around an average value of 90.53 ± 1.57 $W \cdot m^{-2} \cdot °C^{-1}$ in all experimental conditions analyzed, which is comparable to the figures reported for other food products dried under forced convection (Ratti & Crapiste, 1995). Consequently, the application of ultrasound had no significant ($p > 0.05$) impact on either the thermal diffusivity or the heat transfer coefficient. As mentioned above, evidence has previously been reported of the ability of airborne ultrasound to promote heat transport during convective drying. For example, in the aforementioned study by Bantle and Hanssler (2013) on cod drying, the authors identified that the heat transfer coefficient increased from 21.50 to 27.50 $W \cdot m^{-2} \cdot °C^{-1}$ when airborne ultrasound was applied. However, a more pronounced increase, from 10.61 to 24.54 $W \cdot m^{-2} \cdot °C^{-1}$, was reported by Tao et al. (2021) during the airborne ultrasound-assisted drying of blackberry. In this context, it is worth emphasizing once more that ultrasound effects are strongly influenced by the inherent characteristics of the material. These properties govern both the propagation of ultrasonic waves and the resulting effects, as previously elucidated (Ozuna et al., 2014b). As pork liver shrinks during drying, ultrasonic impedance increases because ultrasonic waves propagate faster as moisture content decreases in a harder sample. This results in a greater impedance mismatch between the air and the sample, reducing the transmission coefficient at the interface. Additionally, the interface area for heat and mass transport, as well as for acoustic energy transfer, is modified as drying progresses. Thereby, future investigations should incorporate a more comprehensive model, addressing aspects such as heat energy generation, latent heat of water vaporization, and sample modifications during drying. Assuming all these approaches would refine mathematically modeling and enhance the analysis of heat and transport phenomena.

Conclusions

The application of airborne ultrasound during the convective drying of pork liver affected both the drying rate and the temperatures of the sample and the air. On the one hand, ultrasound reduced the drying time by up to 30% at 40 °C. On the other hand, a temperature increase of less than 5 °C was observed in both the sample and the air flow when ultrasound was applied. Modeling of moisture transport based on diffusion theory was satisfactory and showed an increase in both effective moisture diffusivity and the convective mass transfer coefficient due to ultrasound application. Meanwhile, the analysis of heat transport through conduction and/or convection mechanisms did not reveal any kinetic effects related to ultrasound, although the model fit was not entirely satisfactory. Therefore, underestimated phenomena such as internal heat generation from ultrasound, sample shrinkage, or latent heat of evaporation, could play a significant role in fully understanding the changes in product temperature during drying.

The manuscript pointed to a weak thermal effect of ultrasound during the convective drying of pork liver, which partially contributes to the improvement in mass transport mechanisms. Thereby, it has to be highlighted that airborne ultrasound application has to be considered as an appropriate non-thermal technology with which to improve at industrial level the convective drying of heat-sensitive materials, such as pork liver.

Author Contribution E.A.S.T.: Software, Modelling, Formal analysis, Writing—Original Draft. A.S.G.: Formal Analysis, Review. B.A.: Experimental investigation. J.B.: Conceptualization, Methodology, Funding. J.B.: Software, Modelling, Supervision. J.V.G.P.: Conceptualization, Supervision, Methodology, Formal Analysis, Review.

Funding Open Access funding provided thanks to the CRUE-CSIC agreement with Springer Nature. The authors express their gratitude for the financial support provided by the "Ministerio de Economía y Competitividad (MINECO)" and the "Instituto Nacional de Investigación y Tecnología Agraria y Alimentaria (INIA)" in Spain (Project RTA2017-00024-C04-03). Eduardo A. Sanchez-Torres acknowledges the FPU PhD contract (FPU18/01439) awarded by the "Ministerio de Ciencia, Innovación y Universidades" in Spain.

Data Availability No datasets were generated or analysed during the current study.

Declarations

Competing Interests The authors declare no competing interests.

References

Abbas, K. A., Abdulkarim, S. M., & Jamilah, B. (2008). Thermophysical properties of some species of Malaysian freshwater fish in unfrozen state. *Journal of Food, Agriculture and Environment*, *6*(2), 14–18. https://www.scopus.com/inward/record.uri?eid=2-s2.0-52949093561&partnerID=40&md5=fcf3d7775fc69e4c96857addb207967e. Accessed 30 Nov 2024.

Abril, B., Sánchez-Torres, E. A., Bou, R., Benedito, J., & García-Pérez, J. V. (2022a). Influence of pork liver drying on ferrochelatase activity for zinc protoporphyrin formation. *LWT, 171*, 114128. https://doi.org/10.1016/j.lwt.2022.114128

Abril, B., Sánchez-Torres, E. A., Toldrà, M., Benedito, J., & García-Pérez, J. V. (2022b). Physicochemical and techno-functional properties of dried and defatted porcine liver. *Biomolecules*, *12*(7). https://doi.org/10.3390/biom12070926

Andrés, R. R., Riera, E., Gallego-Juárez, J. A., Mulet, A., García-Pérez, J. V., & Cárcel, J. A. (2019). Airborne power ultrasound for drying process intensification at low temperatures: Use of a stepped-grooved plate transducer. *Drying Technology*. https://doi.org/10.1080/07373937.2019.1677704

Ayadi, M. A., Makni, I., & Attia, H. (2009). Thermal diffusivities and influence of cooking time on textural, microbiological and sensory characteristics of turkey meat prepared products. *Food and Bioproducts Processing, 87*(4), 327–333. https://doi.org/10.1016/j.fbp.2009.03.002

Bantle, M., & Eikevik, T. M. (2014). A study of the energy efficiency of convective drying systems assisted by ultrasound in the production of clipfish. *Journal of Cleaner Production, 65*, 217–223. https://doi.org/10.1016/j.jclepro.2013.07.016

Bantle, M., & Hanssler, J. (2013). Ultrasonic convective drying kinetics of clipfish during the initial drying period. *Drying Technology, 31*(11), 1307–1316. https://doi.org/10.1080/07373937.2013.792093

Cárcel, J. A., García-Pérez, J. V., Riera, E., & Mulet, A. (2007). Influence of high-intensity ultrasound on drying kinetics of persimmon. *Drying Technology, 25*(1), 185–193. https://doi.org/10.1080/07373930601161070

Clemente, G., Bon, J., Sanjuán, N., & Mulet, A. (2011). Drying modelling of defrosted pork meat under forced convection conditions. *Meat Science, 88*(3), 374–378. https://doi.org/10.1016/j.meatsci.2011.01.012

Colucci, D., Fissore, D., Rosselló, C., & Cárcel, J. A. (2018). On the effect of ultrasound-assisted atmospheric freeze-drying on the antioxidant properties of eggplant. *Food Research International, 106*, 580–588. https://doi.org/10.1016/j.foodres.2018.01.022

Contreras, M., Benedito, J., Bon, J., & García-Pérez, J. V. (2018). Intensification of heat transfer during mild thermal treatment of dry-cured ham by using airborne ultrasound. *Ultrasonics Sonochemistry, 41*, 206–212. https://doi.org/10.1016/j.ultsonch.2017.09.019

Cruz, L., Clemente, G., Mulet, A., Ahmad-Qasem, M. H., Barrajón-Catalán, E., & García-Pérez, J. V. (2016). Air-borne ultrasonic application in the drying of grape skin: Kinetic and quality considerations. *Journal of Food Engineering, 168*, 251–258. https://doi.org/10.1016/j.jfoodeng.2015.08.001

Deng, L., Mujumdar, A. S., Zhang, Q., Yang, X., Wang, J., Zheng, Z., Gao, Z., & Xiao, H. (2019). Chemical and physical pretreatments of fruits and vegetables: Effects on drying characteristics and quality attributes – A comprehensive review. *Critical Reviews in Food Science and Nutrition, 59*(9), 1408–1432. https://doi.org/10.1080/10408398.2017.1409192

Erbay, Z., & Icier, F. (2010). A review of thin layer drying of foods: Theory, modeling, and experimental results. *Critical Reviews in Food Science and Nutrition, 50*(5), 441–464. https://doi.org/10.1080/10408390802437063

Fan, K., Zhang, M., & Mujumdar, A. S. (2017). Application of airborne ultrasound in the convective drying of fruits and vegetables: A review. *Ultrasonics Sonochemistry, 39*, 47–57. https://doi.org/10.1016/j.ultsonch.2017.04.001

García-Pérez, J. V., Ortuño, C., Puig, A., Cárcel, J. A., & Pérez-Munuera, I. (2012). Enhancement of water transport and microstructural changes induced by high-intensity ultrasound application on orange peel drying. *Food and Bioprocess Technology, 5*(6), 2256–2265. https://doi.org/10.1007/s11947-011-0645-0

García-Pérez, J. V., Cárcel, J. A., Simal, S., García-Alvarado, M. A., & Mulet, A. (2013). Ultrasonic intensification of grape stalk convective drying: Kinetic and energy efficiency. *Drying Technology, 31*(8), 942–950. https://doi.org/10.1080/07373937.2012.716128

García-Pérez, J. V., Rosselló, C., Cárcel, J. A., De la Fuente, S., & Mulet, A. (2006). Effect of air temperature on convective drying assisted by high power ultrasound. In *Defect and diffusion forum* (Vol. 258, pp. 563–574). Trans Tech Publications Ltd. https://doi.org/10.4028/www.scientific.net/DDF.258-260.563

García-Pérez, J. V., Cárcel, J. A., Mulet, A., Riera, E., Andrés, R. R., & Gallego-Juárez, J. A. (2023). Ultrasonic drying for food preservation. In J. A. Gallego-Juárez, K. F. Graff, & M. B. T.-P. U. (Second E. Lucas (Eds.), *Woodhead Publishing Series in electronic and optical materials* (pp. 743–771). Woodhead Publishing. https://doi.org/10.1016/B978-0-12-820254-8.00027-0

Henchion, M., & McCarthy, M. (2019). Facilitators and barriers for foods containing meat coproducts. In C. Galanakis (Ed.), *Sustainable Meat Production and Processing* (pp. 237–250). Academic Press. https://doi.org/10.1016/B978-0-12-814874-7.00012-2

Jadhav, H. B., Annapure, U. S., & Deshmukh, R. R. (2021). Non-thermal technologies for food processing. *Frontiers in Nutrition, 8*, 657090. https://doi.org/10.3389/fnut.2021.657090

Jakevičius, L., & Demčenko, A. (2008). Ultrasound attenuation dependence on air temperature in closed chambers. *Ultragarsas*, *63*(1), 18–22. https://www.ultragarsas.ktu.lt/index.php/USnd/article/view/17057. Accessed 30 Nov 2024.

Kowalski, S. J. (2018). Intensification of drying processes due to ultrasound enhancement. *Chemical and Process Engineering*, *39*(No 3), 251–262. https://doi.org/10.24425/122947

Llauger, M., Arnau, J., Albano-Gaglio, M., Bover-Cid, S., Martín, B., & Bou, R. (2023). Utilization of porcine livers through the formation of Zn-protoporphyrin pigment optimized by a response surface methodology. *Foods*, *12*(9). https://doi.org/10.3390/foods12091903

Llavata, B., García-Pérez, J. V., Simal, S., & Cárcel, J. A. (2020). Innovative pre-treatments to enhance food drying: A current review. *Current Opinion in Food Science, 35*, 20–26. https://doi.org/10.1016/j.cofs.2019.12.001

Llavata, B., Femenia, A., Clemente, G., & Cárcel, J. A. (2024). Combined effect of airborne ultrasound and temperature on the drying kinetics and quality properties of kiwifruit (Actinidia deliciosa). *Food and Bioprocess Technology, 17*(2), 440–451. https://doi.org/10.1007/s11947-023-03138-6

Miano, A. C., Ibarz, A., & Augusto, P. E. D. (2016). Mechanisms for improving mass transfer in food with ultrasound technology: Describing the phenomena in two model cases. *Ultrasonics Sonochemistry, 29*, 413–419. https://doi.org/10.1016/j.ultsonch.2015.10.020

Mieszczakowska-Frąc, M., Dyki, B., & Konopacka, D. (2016). Effects of ultrasound on polyphenol retention in apples after the application of predrying treatments in liquid medium. *Food and Bioprocess Technology, 9*(3), 543–552. https://doi.org/10.1007/s11947-015-1648-z

Miraei Ashtiani, S., Rafiee, M., Mohebi Morad, M., & Martynenko, A. (2022). Cold plasma pretreatment improves the quality and nutritional value of ultrasound-assisted convective drying: The case of goldenberry. *Drying Technology, 40*(8), 1639–1657. https://doi.org/10.1080/07373937.2022.2050255

Muga, F. C., Workneh, T. S., & Marenya, M. O. (2020). Modelling the thin-layer drying of beef biltong processed using hot air drying. *Journal of Biosystems Engineering*. https://doi.org/10.1007/s42853-020-00076-5

Mujaffar, S., & Sankat, C. K. (2015). Modeling the drying behavior of unsalted and salted catfish (Arius sp.) slabs. *Journal of Food Processing and Preservation, 39*(6), 1385–1398. https://doi.org/10.1111/jfpp.12357

Musielak, G., & Mierzwa, D. (2021). Enhancement of convection heat transfer in air using ultrasound. *Applied Sciences*, *11*(19). https://doi.org/10.3390/app11198846

Nesvadba, P., & Eunson, C. (1984). Moisture and temperature dependence of thermal diffusivity of cod minces. *International Journal of Food Science & Technology, 19*(5), 585–592. https://doi.org/10.1111/j.1365-2621.1984.tb01875.x

Ozuna, C., Cárcel, J. A., Walde, P. M., & García-Pérez, J. V. (2014a). Low-temperature drying of salted cod (Gadus morhua) assisted by high power ultrasound: Kinetics and physical properties. *Innovative Food Science & Emerging Technologies, 23*, 146–155. https://doi.org/10.1016/j.ifset.2014.03.008

Ozuna, C., Gómez Álvarez-Arenas, T., Riera, E., Cárcel, J. A., & García-Pérez, J. V. (2014b). Influence of material structure on airborne ultrasonic application in drying. *Ultrasonics Sonochemistry, 21*(3), 1235–1243. https://doi.org/10.1016/j.ultsonch.2013.12.015

R Core Team. (2022). *R: A language and environment for statistical computing*. https://www.r-project.org/. Accessed 30 Nov 2024.

Ratti, C., & Crapiste, G. H. (1995). Determination of heat transfer coefficients during drying of foodstuffs. *Journal of Food Process Engineering, 18*(1), 41–53. https://doi.org/10.1111/j.1745-4530.1995.tb00353.x

Rinaldi, M., Chiavaro, E., & Massini, R. (2010). Apparent thermal diffusivity estimation for the heat transfer modelling of pork loin under air/steam cooking treatments. *International Journal of Food Science & Technology, 45*(9), 1909–1917. https://doi.org/10.1111/j.1365-2621.2010.02360.x

Rodríguez, O., Santacatalina, J. V., Simal, S., García-Pérez, J. V., Femenia, A., & Rosselló, C. (2014). Influence of power ultrasound application on drying kinetics of apple and its antioxidant and microstructural properties. *Journal of Food Engineering, 129*, 21–29. https://doi.org/10.1016/j.jfoodeng.2014.01.001

Sánchez-Torres, E. A., Abril, B., Benedito, J., Bon, J., & García-Pérez, J. V. (2021). Water desorption isotherms of pork liver and thermodynamic properties. *LWT, 149*, 111857. https://doi.org/10.1016/j.lwt.2021.111857

Sánchez-Torres, E. A., Abril, B., Benedito, J., Bon, J., Toldrà, M., Parés, D., & García-Pérez, J. V. (2022). Airborne ultrasonic application on hot air-drying of pork liver. Intensification of moisture transport and impact on protein solubility. *Ultrasonics Sonochemistry, 86*, 106011. https://doi.org/10.1016/j.ultsonch.2022.106011

Tao, Y., Li, D., Siong Chai, W., Show, P. L., Yang, X., Manickam, S., Xie, G., & Han, Y. (2021). Comparison between airborne ultrasound and contact ultrasound to intensify air drying of blackberry: Heat and mass transfer simulation, energy consumption and quality evaluation. *Ultrasonics Sonochemistry, 72*, 105410. https://doi.org/10.1016/j.ultsonch.2020.105410

Theußl, S., Schwendinger, F., & Hornik, K. (2017). ROI: The R optimization infrastructure package (issue 133). https://doi.org/10.57938/08a09f34-9a68-42ad-9218-0bbaa624cc61

Villamiel, M., Riera, E., & García-Pérez, J. V. (2021). The use of ultrasound for drying, degassing and defoaming of foods. In *Innovative food processing technologies: A comprehensive review* (pp. 415–438). Elsevier. https://doi.org/10.1016/b978-0-08-100596-5.22957-0

Wakamatsu, J. (2022). Evidence of the mechanism underlying zinc protoporphyrin IX formation in nitrite/nitrate-free dry-cured Parma ham. *Meat Science, 192*, 108905. https://doi.org/10.1016/j.meatsci.2022.108905

Yao, Y. (2016). Enhancement of mass transfer by ultrasound: Application to adsorbent regeneration and food drying/dehydration. *Ultrasonics Sonochemistry, 31*, 512–531. https://doi.org/10.1016/j.ultsonch.2016.01.039